

## SUPPLEMENTARY INFORMATION

### **Solving Hierarchical Helical Mesostructures by Electron Tomography**

Pei Yuan,<sup>a,b</sup> Lingzhi Zhao,<sup>a</sup> Nian Liu,<sup>a</sup> Guangfeng Wei,<sup>a</sup> Yunhua Wang,<sup>a</sup> Graeme J. Auchterlonie,<sup>c</sup> J. Drennan,<sup>c</sup> Gao Qing Lu,<sup>d</sup> Jin Zou,<sup>\*b,c</sup> and Chengzhong Yu<sup>\*a,d</sup>

*a Department of Chemistry and Shanghai Key Laboratory of Molecular Catalysis and Innovative Materials, Fudan University, Shanghai, 200433, P. R. China. Tel: +86-21-55665103; E-mail: Email: czyu@fudan.edu.cn*

*b School of Engineering, The University of Queensland, Brisbane, QLD 4072, Australia. E-mail: j.zou@uq.edu.au*

*c Centre for Microscopy and Microanalysis, The University of Queensland, Brisbane, QLD 4072, Australia*

*d ARC Centre of Excellence for Functional Nanomaterials and Australian Institute for Bioengineering and Nanotechnology, The University of Queensland, Brisbane, QLD 4072, Australia.*

## Synthesis Methods and Characterization

All chemicals were used as received without further purification. Otadecyltrimethyl ammonium bromide ( $C_{18}$ TAB) and perfluorooctanoic acid (PFOA) were purchased from Aldrich. Other chemicals were purchased from the Shanghai Chemical Company. Mesostructured material was synthesized under basic conditions by using  $C_{18}$ TAB as a template and PFOA as an additive. In a typical synthesis, 0.20 g of  $C_{18}$ TAB was dissolved in 96 g of deionized water by stirring at room temperature. Then, 0.70 mL of NaOH (2 M) and 0.01 g of PFOA were added separately into the solution. The temperature of the solution was raised to 80 °C. To this solution, 1.34 mL of tetraethyl orthosilicate (TEOS) was added with continuously stirring. The mixture was then stirred for additional 2 h. The solid products were then collected by filtration, washed with de-ionized water, and dried in air at room temperature. The as-synthesized samples were calcined at 550 °C for 5 h in air to remove the templates. In this one-pot synthesis, various mesostructures, including HH rods and concentric circular mesostructures and so on, has been synthesized. Here we focused only on the direct determination of the pitch and chirality of HH rods.

ET was performed using a FEI Tecnai F30 electron microscope operating at 300 kV. All TEM images were recorded at a given defocus in a bright-field mode to show the thickness contrast. The ET specimens were prepared by dispersing the powder samples in ethanol by ultrasonication for 5 min and then depositing them directly onto copper grids (2000×1000 slot, Proscitech) with Formvar supporting films. Colloidal gold particles (5 nm) were deposited on both surfaces of the grid as fiducial markers for the subsequent image alignment procedures. The tomographic tilt series were carried out by tilting the specimen inside the microscope around a dual axis under the electron beam. 121 projected TEM images were recorded over a tilt range of +60° to -60° at increments of 1°. Images of the tilt-series were aligned with respect to a common origin and rotation axis using the fiducial markers. Alignment and three-dimensional reconstructions of HH structures by filtered back projection were performed with IMOD and AMIRA software.<sup>1,2</sup> The models were simulated using the 3ds max software (Autodesk).

### The quantitative explanation for the definition of the fringes.

As shown in the schematic model (Fig. 3c), the projected area ( $Sp$ ) of (10) planes (originally a hexagonal section) to y-z plane can be used to quantify the location and legibility of fringes, where smaller  $Sp$  corresponds to a smaller derivation of the view direction from the [10] direction and thus a more legible fringe is observed. The external helix (the micelle in the center) can be described by the following parameter equation

$$\begin{cases} x = R \cos t \\ y = R \sin t \\ z = C \cdot t \end{cases}, \quad (1)$$

where  $t$  is the phase angle,  $R$  is the radius of external helix, and  $C = Ps / 2$  ( $Ps$  is the pitch of the external helix).

$Sp$  can then be calculated by the equation

$$S_p = S_0 \cdot \cos \theta \cdot \sin t = S_0 \cdot \frac{R}{\sqrt{R^2 + C^2}} \cdot \sin t, \quad (2)$$

where  $\theta$  is the tilt angle of the external helix to x-y plane and  $S_0$  is the hexagonal cross section area (Fig. 3a), a constant for a given rod with uniform diameter.

From Equation (2), it can be seen that  $t$  and  $\theta$  are two key factors to determine the positions where the original observable fringes can be retained or become blurred or even disappear. The deduction can be inferred that at phase angle  $t = n\pi$ ,  $Sp = 0$ , and the fringes can be clearly observed in this case, while at other phase angles,  $Sp \neq 0$ , so that the original observable fringes should become less resolved or even disappear.

On the other hand,  $\theta$  increases as  $R$  is decreased and  $C$  is increasing. Thus the HH rod with small  $R$  and large  $C$ , the fringes at both special (0 and  $\pi$ ) and non-special positions ( $\pi/3$ ,  $2\pi/3$ ,  $4\pi/3$ ,  $5\pi/3$ ) can be observed but a little blurred at the non-special sections (as shown in Fig. S1a). In the case of HH rod with small  $C$ , only the fringes in the two specific positions (0 and  $\pi$ ) in one  $Ps$  can be clearly observed (Fig. S1c).

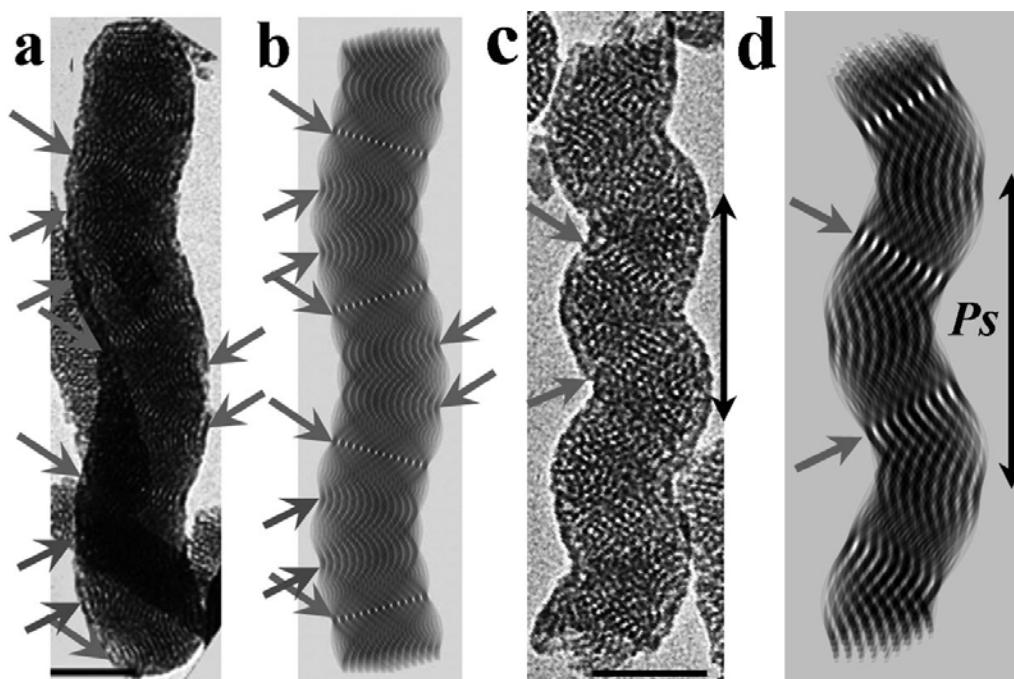


**Fig.S1** The TEM images of HH rods with small  $R$  and large  $P_s$  (a) and small  $P_s$  (c) and their corresponding simulated projective images (b and c, respectively) showing the definition of the (10) fringes (indicated by the arrows). The clear fringes are located at the specific positions ( $0$  and  $\pi$ ).

## References

1. Kremer, J. R.; Mastronarde, D. N.; McIntosh, J. R. *J. Struct. Biol.* **1996**, *116*, 71-76.
2. AMIRA homepage: <http://www.tgs.com/products/amira.asp>.